Results in Engineering 11 (2021) 100273

Contents lists available at ScienceDirect

Results in Engineering

journal homepage: www.sciencedirect.com/journal/results-in-engineering

The experimental investigation of hardness and wear behaviors of inner surface of the resin tubes reinforced by fibers

Kaveh Rahmani [a,*], Greg Wheatley [b], Ali Sadooghi [e], Seyed Jalal Hashemi [c], Jafar Babazadeh [d]

[a] Department of Mechanical Engineering, Bu-Ali Sina University, Hamedan, Iran
[b] College of Science & Engineering, James Cook University, James Cook Dr, Douglas, QLD, 4811, Australia
[e] Department of Mechanical Engineering, Shahid Rajaee Teacher Training University, Tehran, Iran
[c] Department of Mechanical Engineering, Faculty of Enghelab-e Eslami, Technical and Vocational University (TVU), Tehran, Iran
[d] Department of Mechanical Engineering, Kar Higher Education Institute of Qazvin, Qazvin, Iran

ARTICLE INFO

Keywords:
Composite tube
Reinforcement fiber
Hardness
Wear behavior

ABSTRACT

Resin tubes made of epoxy base material and fibers are widely used in the transportation, and aeronautics industries due to their high mechanical properties. Different reinforcing fibers and resins are usually used in making these tubes and lead to various properties. In this study, tubes made by using a 45-degree unilateral winding method and reinforced by Glass, Carbon, and Kevlar fibers and their hardness and wear behaviors were investigated. The results showed that the highest hardness was obtained for the carbon fiber reinforced composite tube (CFR), equal to 65HV, which was 109% more than the Kevlar fiber reinforced composite tube (KFR). Higher hardness indicates greater resistance of the material to local deformation and also stronger bonding between the base material and the reinforcing fibers. The wear test results showed that the wear rate of CFR was 6 mg/m, which was 26% and 55% lower than the glass fiber reinforced composite tube (GFR) and KFR, respectively. The obtained result can be explained as a result of good bonding and compatibility between carbon fibers and used resin. Scanning electron microscope (SEM) images were taken to evaluate the results.

1. Introduction

Polymeric composite materials involve polymer and fibers and have a high strength to weight ratio as well as low density, rigidity, high tensile and flexural strength [1,2]. In this type of composite, the reinforcing phase is combined with the base material, which is a thermoset or thermoplastic polymer [3]. The properties of polymeric composites depend on the polymer properties as well as on the type, direction, and length of the fibers and the quality of resin and fiber bonding [4]. Fibers in the industry are divided into two categories of synthetic and natural fibers; which often have high elastic modulus and are embedded in the polymer matrix and the roles of fibers are transferring forces to themselves, absorbing energy, and improving toughness [5]. The vinyl ester, phenol-formaldehyde epoxy, and poly amid resins are the most commonly used among the thermoset polymers [6]. Carbon fibers are cyclic organic that forms a tough, impact-resistant structure [7]. Kevlar fibers are made from long molecular chains that have good thermal stability and wear resistance [8]. Due to the raw materials and the production process, the inner surface of these tubes is smooth, which reduces energy consumption, and the friction coefficient allows it to not require pipe protection against corrosive factors [9]. Jelf et al. [10] produced carbon-fiber epoxy samples and their strength was calculated under combined compression and shear loading. The major reason for samples' failure was as a result of plastic micro buckling. Moshir et al. [11] conducted a study on the mechanical properties of fiber-reinforced composite tubes. The results of the tests showed that the KFR withstands more shear stress than the other tubes. Khomejani et al. [12] studied the mechanical and tensile properties of GFR and the results showed that different weight percentages and different directions of fibers resulted in different properties for composite tubes. Fibers' arrangement and their compatibility and interleaving with resin play a vital role in the determining of the resin tube properties [13]. Rahmani et al. [14] produced Polymeric tubes by using a 45-degree unilateral winding method and their corrosion and creep properties were investigated. The highest creep strain was obtained for the CFR equal to 0.7445 and the lowest was obtained for KFR with the Kevlar fibers being severely damaged. Ren et al. [15] produced a polymer composite tube reinforced by carbon fibers in which carbon fibers were wound with $\pm 45^{\circ}$ and a compression

* Corresponding author.
E-mail address: rahmanii.kaveh@gmail.com (K. Rahmani).

https://doi.org/10.1016/j.rineng.2021.100273
Received 3 July 2021; Received in revised form 7 August 2021; Accepted 17 August 2021
Available online 23 August 2021

test was done on them. By increasing pressure force, less buckling load was obtained. At a similar investigation, Yang et al. [16] analyzed the creep rate of the composite tubes under flexural loading at 100 °C for 500 h. The result showed that the service reliability achieved a 12-year design life.

As a result of a good interface, compatibility, and adhesion between fibers and resins, it helps in effective load transfer, and on the contrary, it leads to problems in material performance and delamination. The chemical structure, molecular weight, and distribution play a vital role in delamination. Laboratory investigation is the common way to determine the compatibility of fiber reinforcement materials [14].

In this manuscript, resin tubes with polymer base-material were reinforced by fibers. All the fibers were glass, carbon, and Kevlar and were wound at angle ±45° degrees. Also, the main point of the manuscript is using different resins for various fibers by considering the compatibility role by choosing the appropriate resin for each fiber. After tube production, the microhardness and pin on disk wear test have been done on them to investigate their resistance against plastic deformation and the achieved results were corroborated by taking SEM images.

2. Experiments

2.1. Materials and producing tubes

As mentioned, the various resins were used for fibers with the aim of producing high-quality tubes. The Swancor-901, Epiran-10, and Epiran-06FL resins were mixed with fibers in GFR, CFR, and KFR production [1]. To facilitate the curing process as well as better bonding between resins and fibers, cobalt actuate solution with DMA126 technical specification and peroxide acid solution with MEKP101 technical specification were added to the resin at 1.5% and 15% by weight, respectively [18]. All the materials were mixed for 60min in a stirring machine and after that fibers were immersed in the resins for 20min. All the fibers have a plain-woven structure and their physical and mechanical properties are shown in Table 1.

The winding machine included a shaft with a 26 mm diameter called a mandrel that, the mixture of fibers and resins wound around the mandrel. The mandrel was polished and a gel coat layer was sprayed with a thickness of 0.7 mm to achieve smoothness and proper adhesion. Table 2 presents the specifications and layering fibers of the tubes.

After wrapping, the tubes were placed for 2h at ambient temperature for initial curing and then were placed in an oven for 2h at 70 °C for final curing. Fig. 1 shows a produced tube and, their dimensional characteristics are given in Table 3. All the tubes have 3.34 mm average thickness and 33.4 mm average diameter.

2.2. Determining mechanical properties

To investigate the impact of used fibers as a reinforcement in the composite tubes, hardness and wear tests were done on them as follows. The Vickers microhardness test was performed on the samples with 5 repetitions according to ASTM-D4762 standard, and 15N force by a 1/16 in diameter penetrant tool [19]. The pin on disk wear test was also performed on the inner surface of the produced tubes according to the specifications of Table 4 and ASTM G99 standard [20]. The wear test setup and the graphical procedure are shown in Fig. 2 and Fig. 3.

Table 1
The detailed specification of used fibers.

Fiber	Thickness (μm)	Density (g/cm3)	Break Elongation (%)	Specific Tensile Strength (Glb/in^2)
Glass	10	2.54	4.8	5.43
Carbon	15	1.79	1.4	6.93
Kevlar49	15	1.43	2.4	7.38

Table 2
The feature and arrangements of fibers for production tubes.

Sample	Inner Layer		Middle Layer		Outer Layer	
	Material	Mark	Material	Mark	Material	Mark
GFR	Glass Fiber	Mat225	Glass Fiber	Woven 600	Glass Fiber	Mat225
CFR	Fabric	Re300	Carbon Fiber	300	Fabric	Re300
KFR	Fabric	Re300	Kevlar Fiber	49	Fabric	Re300

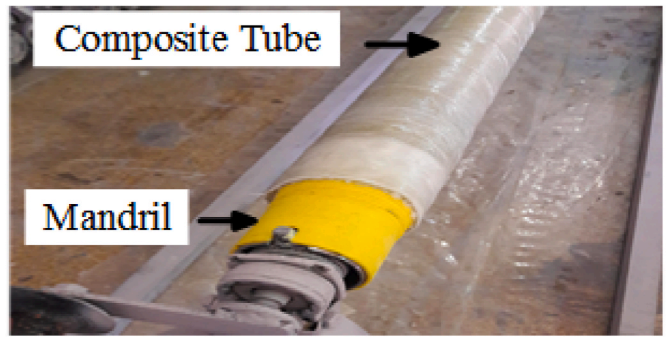

Fig. 1. The produced composite tube.

Table 3
The specification of the produced tubes.

Sample	Mass per 20 cm (g)	Density (g/mm3)
GFR	79	1.252
CFR	75	1.189
KFR	78	1.237

Table 4
The specification of the wear test.

Radius (mm)	Angular velocity (rpm)	Distance (m)	Time (min)	Velocity (m/s)	Force (N)
4	225	300	20	0.1	10

3. Results and discussion

3.1. Specification of samples

Fig. 4 shows the images of the cut samples on which the hardness and wear tests were performed with SEM images of the samples' cross-section to ensure the quality of adhesion and compatibility between the epoxy base material and the fibers. As can be seen, there are not any discontinuities, porosities, or cavities in the samples, which are common defects in fiber reinforcement samples.

To clarify the crystalline structure of the produced samples, the X-ray diffraction (XRD) pattern was provided which was shown in Fig. 5. No new phases were created after production as well as no interaction phases.

3.2. The microhardness test

The microhardness test results of the samples are shown in Table 5 and the average microhardness in Fig. 6. In this experiment, the penetrating force was applied perpendicular to the fiber length. There was no significant difference between the 5 results of each sample. The small difference between the results can be due to the location of the applied penetrating force, whether it is applied precisely to the reinforcing fibers

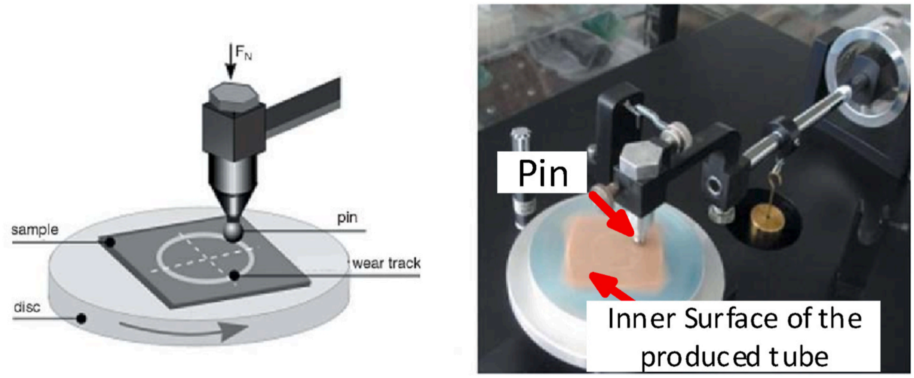

Fig. 2. The setup of the wear test.

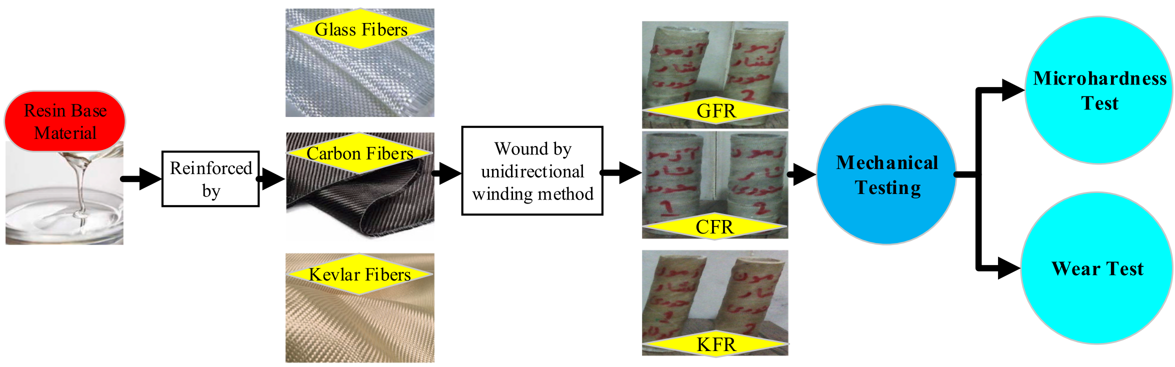

Fig. 3. The graphical procedure.

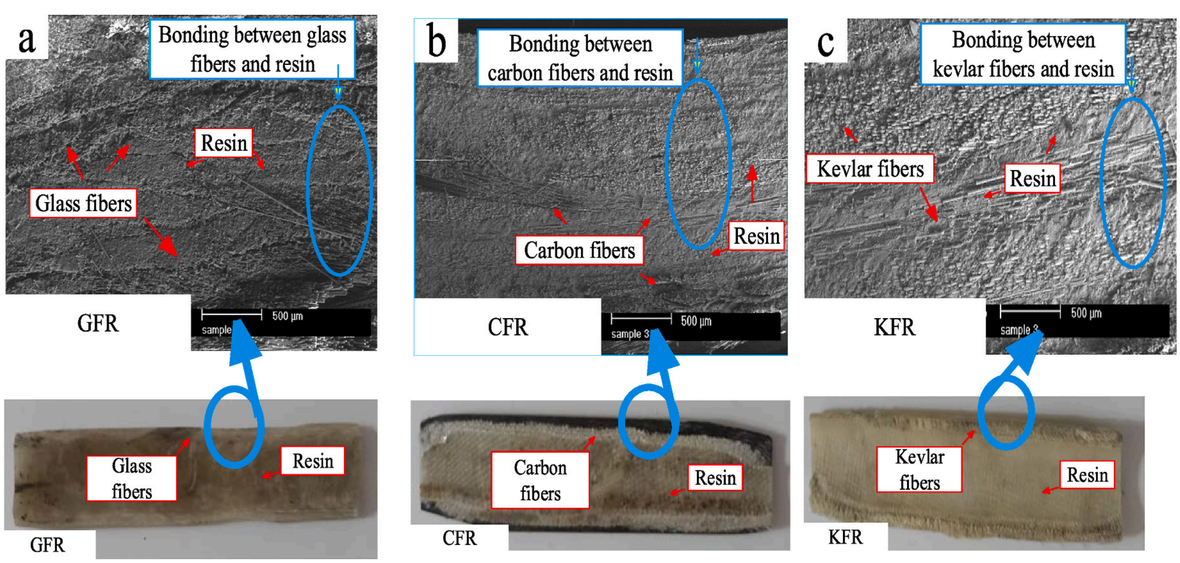

Fig. 4. The SEM images of the cross-section of samples.

or between the fibers and the base material.

Also, the results show that the highest microhardness was obtained for CFR, equal to 65HV, which is 27% more than GFR. The lowest hardness was achieved for KFR equal to 31HV. Higher hardness indicates greater resistance of the material to local deformation and also indicates a stronger bonding between the base material and the reinforcing fibers. The hardness of produced fiber reinforcement composite samples depends on various factors such as the fiber's layout and type, fraction percentage of fiber, base resin hardness, and the bond between the fibers and the base material [21]. On the other hand, carbon fibers' higher hardness compared to other fibers has led to this result. When applying force to composite samples, reinforcing fibers play the most important role in tolerating and diverting the force, resulting in less force being applied to the resin base material. In general, the material's resistance to deformation and force penetration is proportional to its modulus of elasticity [22]. Also, since the modulus of elasticity of carbon fibers is higher than other used fibers to produce samples, it results in the production of composite samples with higher hardness. Another case

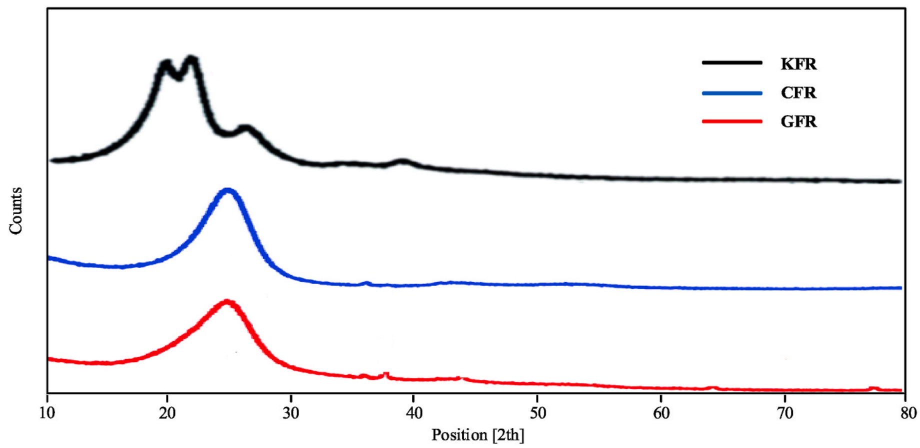

Fig. 5. The XRD pattern of the produced samples.

Table 5
The results of microhardness.

Sample	HV1	HV2	HV3	HV4	HV5
GFR	48.7	42.0	49.2	56.2	58.7
CFR	65.9	65.6	65.3	65.4	63.0
KFR	27.6	24.8	30	36.8	36.3

study related to the hardness of the produced samples is the increase in hardness for the used resin base-material for each sample. Due to the different resins used with different fibers, as a result of the compatibility role, the hardness of the raw materials varies. In the present study, the layout of the fiber in the composite tubes was the same. The hardness of pure base resin without fibers, after curing operation was compared with the average hardness of produced samples in Table 6.

According to the results, it is observed that the highest percentage of reinforcement was caused by carbon fibers equal to 44%. The higher difference in the hardness between the base resin and its composite means the proper distribution of fibers, and the proper bonding between fibers and the resin. In fact, with the uniform distribution of the applied force between the fibers, higher resistance to plastic deformation is created. On the other hand, the lowest hardness was obtained for KFR, which only improved the hardness of its resin by 14%, indicating poor bond quality between these fibers and its resin. An increase of 34% in the hardness of the GFR's resin indicates a proper bonding between glass fibers and its resin.

3.3. The wear test

Wearing parts and equipment play an important role in wear and erosion mechanisms. The wear test was performed on the samples based on the 300 m pin movement. The results of the wear test, including the wear rate and friction coefficient of the samples, are visible in Table 7 and Fig. 7.

The wear test results show that the lowest wear was obtained for CFR, equal to 6 mg/m, which is 55% lower than the wear rate of KFR. In contrast, Kevlar fibers have the highest wear rate equal to 9.3 mg/m due to their weaker mechanical properties. Wear resistance is a function of two mechanical properties of hardness and toughness that by increasing

Table 6
The comparison of hardness between the pure resin and produced sample.

Sample	Used resin	Hardness of resin	Hardness of sample	% of hardness increase
GFR	Swancor-901	38	51	34
CFR	Epiran-10	45	65	44
KFR	Epiran-06FL	27	31	14

Table 7
The results of the wear test.

Sample	Initial mass (g)	Final mass (g)	Loss mass (g)	Ave. friction coefficient	Ave. friction force (N)	Wear rate (mg/m)
GFR	5.3	3	2.3	0.157	1.57	7.6
CFR	5	3.2	1.8	0.128	1.28	6
KFR	5.2	2.4	2.8	0.243	2.43	9.3

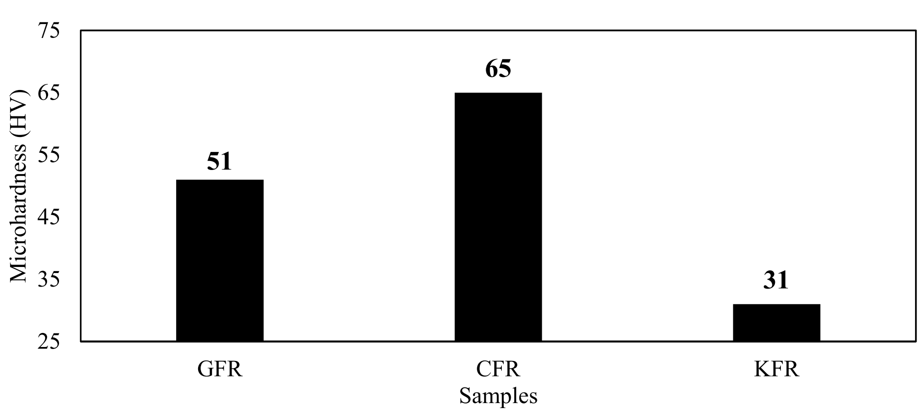

Fig. 6. The graph of average microhardness results.

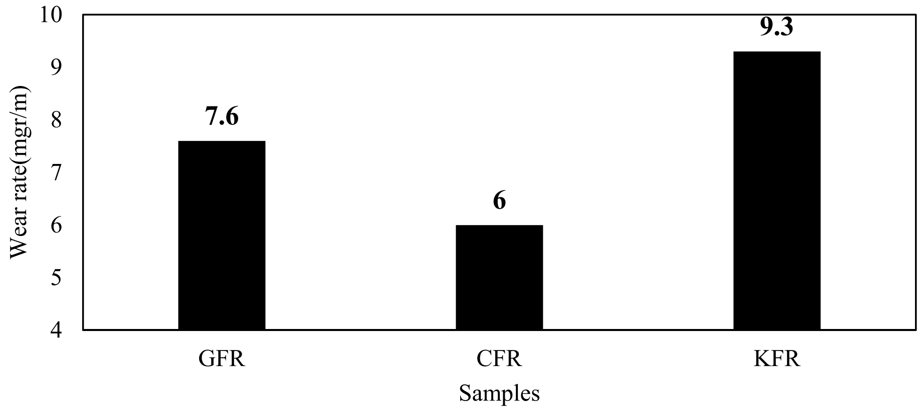

Fig. 7. The graph of wear rate samples' results.

these properties, the wear resistance is further increased, resulting in less plastic deformation and a lower wear rate and friction coefficient. According to the microhardness results, the highest hardness was obtained for CFR, and the lowest wear rate also corresponded to this sample. The obtained result can be explained as a result of good bonding and compatibility between carbon fibers and used resin. The other output of the wear test is the weight loss of the samples after the test. The highest value was obtained for KFR equal to 53%, then 43%, and 36% for the GFR and CFR, respectively.

To better investigate the result, SEM images were taken from the worn surfaces, which are visible in Fig. 8. By increasing the wear rate, the number and depth of grooves in the samples increased as well as the plastic deformation. Also, due to the pin movement on the samples, the fibers were damaged severely and due to the applied force, the fibers lost their bonding with the resin and were easily disrupted. Also, Fig. 6 shows de-bonding and plastic deformation as well as wear tracks such that abrasion and delamination are the dominant wear mechanisms in the worn surfaces. As illustrated in Fig. 8, in the worn surface of KFR, more separated and high plastic deformation and de-bonding are observed compared to CFR and GFR. These features along with plastic deformation indicate adhesive and delamination wear mechanisms in the worn surfaces.

Also, to understand the behavior of the samples against the applied force, the friction coefficient was calculated over the traced distance (300 m), and the graph of the instantaneously generated coefficient of friction on the samples is visible in terms of distance (Fig. 9). According to the compatibility role, a fabric Re300 was used in the outer layers to obtain better bonding between resins and carbon fibers in CFR and Kevlar fibers in the KFR samples. The used fabric Re300 is much softer compared to the Kevlar and carbon fibers. During the wear test, the pin rotates on the produced samples and after passing a distance, almost 150 m, the fabric layers were removed and the pin reaches the Kevlar and carbon fibers. The increase of the coefficient of friction after a period of time in the wear test for the CFR and KFR is a result of this matter. Furthermore, after a while, since the base material of the produced samples is polymer and resin, the surface temperature of samples increased and it led to more adhesion between samples and pin, and the coefficient of friction increased. The samples were subjected to thermal load due to the sliding motion and fluctuation of the pin in the wear test [23]. Since the fibers and resins have low thermal conductivity, thermal gradients were generated and the temperature increased in the surface of the pin [24]. The temperature and deformations of the produced samples' surfaces led to increasing the thermal stresses that added to mechanical stress. This procedure can propagate the crack and grooves in the samples [25,26]. The lowest friction coefficient is for CFR, equal to 0.128, which is 22% and 89% lower than GFR and KFR, respectively. This indicates the proper bonding between the carbon fibers and the base material and less tendency to adhere between the ductile plastic layers and the surface during wear. In these diagrams, many oscillations result from repeated adhesion and separation of fibers on the surface of the samples, causing slight changes in the applied force between the pin and the sample.

4. Conclusion

In this study, resin base tubes were reinforced with glass, carbon, and Kevlar fibers with the unidirectional winding method. All the fibers were wound at 45-degree by the winding method. The microhardness and

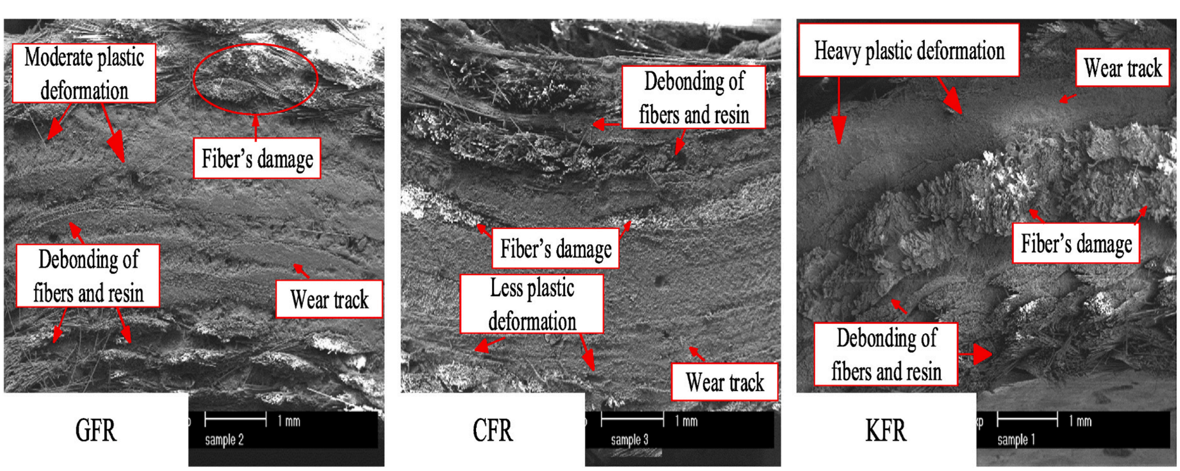

Fig. 8. The SEM images of the worn surface of samples.

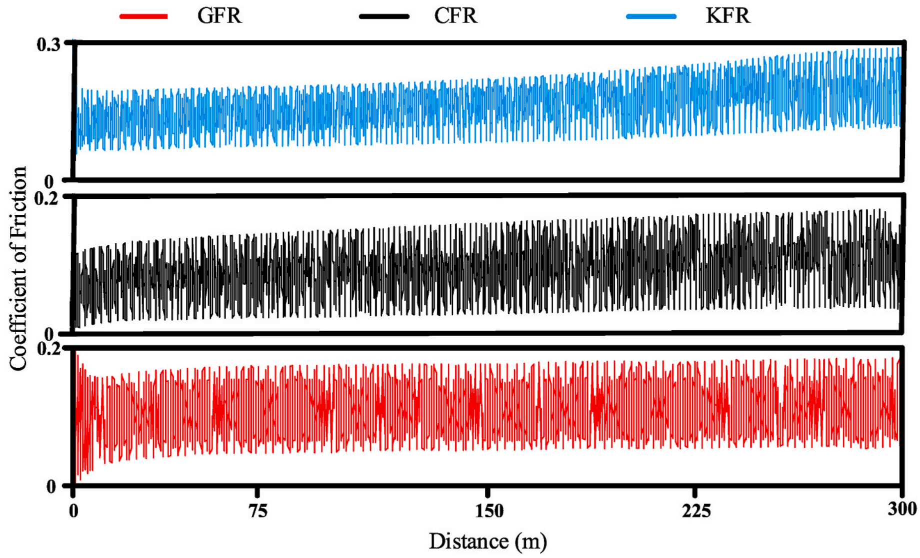

Fig. 9. The Coefficient of friction of the samples.

wear properties of the produced samples were evaluated and the tests were done according to the standard procedure. The obtained results are as follows.

1. The XRD graph showed that no new phases were created after production as well as no interaction phases. It means that the production process is appropriate and the compatibility between resin and fibers is achieved.
2. SEM images of the cross-section and worn samples' surface approved that the bonding and adhesion between resins and fibers were appropriate and there are not any cavities due to the good bonding.
3. The highest hardness equal to 65HV was obtained for CFR, which is 27% and 109% higher than the hardness of GFR and KFR, respectively. Higher hardness indicates greater resistance of the material to local deformation and also indicates a stronger bonding between the base material and the reinforcing fibers.
4. The lowest wear rate was obtained for CFR, equal to 6 mg/m, which is 26% and 55% lower than GFR and KFR, respectively. By increasing the wear rate, the number and depth of grooves in the samples increased as well as the plastic deformation.

Credit author statement

Kaveh rahmani: Conceptualization, Investigation, Supervision. **Greg Wheatley**: Reviewing. **Ali Sadooghi**: Data curation, Visualization, Validation. **Seyed Jalal Hashemid**: Writing- Reviewing and Editing. **Jafar Babazadeh**: Writing- Original draft preparation.

Declaration of competing interest

The authors declare that they have no known competing financial interests or personal relationships that could have appeared to influence the work reported in this paper.

References

[1] Jafar Babazadeh, et al., Effect of glass, carbon, and kevlar fibers on mechanical properties for polymericcomposite tubes produced by unidirectional winding method, Mater. Res. Express (2021).

[2] Hashemi, Seyed Jalal, et al., Investigation on the mechanical behavior of fiber-metal laminates based on polyvinyl chloride reinforced by 3D glass fibers, Materials Today Communications 25 (2020) 101273.

[3] N.S. Kavitha, Raghu V. Prakash, Size scale effects on post-impact residual strength of hybrid glass/carbon/epoxy nano-composites, Procedia materials science 3 (2014) 2134–2141.

[4] Wasim Akram, Sachin Kumar Chaturvedi, Syed Mazhar Ali, Comparative study of mechanical properties of e-glass/epoxy composite materials with Al2O3, CaCo3, SiO2 AND PBO fillers, Int. J. Eng. Res. Technol. 2 (7) (2013) 1029–1034.

[5] Elham Ansari, et al., The effect of middle layer material and thickness on the quasi-static energy absorption of FML, 2018, pp. 427–436.

[6] Paolo Giani, et al., Launch control for sport motorcycles: a clutch-based approach, Contr. Eng. Pract. 21 (12) (2013) 1756–1766.

[7] Patil Deogonda, Vijaykumar N. Chalwa, Mechanical property of glass fiber reinforcement epoxy composites, Int. J. Sci. Eng. Res. 1 (4) (2013) 2347–3878.

[8] G.V. Mahajan, V.S. Aher, Composite material: a review over current development and automotive application, International journal of scientific and research publications 2 (11) (2012) 1–5.

[9] Isaac M. Daniel, et al., Engineering Mechanics of Composite Materials, vol. 3, Oxford university press, New York, 1994.

[10] P.M. Jelf, N.A. Fleck, The failure of composite tubes due to combined compression and torsion, J. Mater. Sci. 29 (11) (1994) 3080–3084.

[11] Saeid Khadem Moshir, et al., Mechanical behavior of thick composite tubes under four-point bending, Compos. Struct. (2020) 112097 [17].

[12] Soheil Khomejani-Farahani, Mojtaba Haghighi-Yazdi, Majid Safarabadi, Numerical study of the effect of torsional fatigue loading on the energy absorption of composite tubes, Polym. Compos. (2019).

[13] A. Gunge, P.G. Koppad, M. Nagamadhu, S.B. Kivade, K.V.S. Murthy, Study on mechanical properties of alkali treated plain woven banana fabric reinforced biodegradable composites, Composites Communications 13 (2019) 47–51.

[14] Kaveh Rahmani, et al., The experimental analysis of creep and corrosion properties of polymeric tube reinforced by glass, carbon and Kevlar fibers, Mater. Res. Express (2021).

[15] Z. Ren, et al., Damage and failure in carbon fiber-reinforced epoxy filament-wound shape memory polymer composite tubes under compression loading, Polym. Test. 85 (2020) 106387.

[16] Z. Yang, et al., Flexural creep tests and long-term mechanical behavior of fiber-reinforced polymeric composite tubes, Compos. Struct. 193 (2018), 154–64.

[18] H.B. Vinay, H.K. Govindaraju, Prashanth Banakar, A review on investigation on the influence of reinforcement on mechanical properties of hybrid composites, Int. J. Pure Appl. Sci. Technol. 24 (2) (2014).

[19] ASTM D4762-18, Standard Guide for Testing Polymer Matrix Composite Materials, ASTM International, West Conshohocken, PA, 2018. www.astm.org.

[20] K. Rahmani, A. Sadooghi, S.J. Hashemi, The effect of Al2O3 content on tribology and corrosion properties of Mg-Al2O3 nanocomposites produced by single and double-action press, Mater. Chem. Phys. (2020) 123058.

[21] Ali Sadooghi, Gholamhassan Payganeh, Effects of sintering process on wear and mechanical behavior properties of titanium carbide/hexagonal boron nitrid/steel 316L base nanocomposites, Mater. Res. Express 5 (2) (2018), 025038.

[22] Kaveh Rahmani, Sadooghi Ali, Mohammad Nokhberoosta, The effect of the double-action pressure on the physical, mechanical and tribology properties of Mg-WO3 nanocomposites, Journal of Materials Research and Technology 9 (1) (2020) 1104–1118.

[23] A. Belhocine, D. Shinde, R. Patil, Thermo-mechanical coupled analysis based design of ventilated brake disc using genetic algorithm and particle swarm optimization, JMST Adv (2021), https://doi.org/10.1007/s42791-021-00040-0.

[24] Belhocine Ali, Oday Ibraheem Abdullah, A thermomechanical modelfor the analysis of disc brake using the finite element method in frictional contact, J. Therm. Stresses (2019), https://doi.org/10.1080/01495739.2019.1683482.

[25] Ali Belhocine, Mostefa Bouchetara, Thermomechanical behavior of dry contacts in disc brake rotor with a grey cast iron composition, Therm. Sci. 17 (2) (2013) 599–609.

[26] Mohd Razmi Ishak, et al., Brake torque analysis of fully mechanical parking brake system: theoretical and experimental approach, Measurement 94 (2016) 487–497.